# Ultra High-Resolution NMR: Sustained Induction Decays of Long-Lived Coherences

Aurélien Bornet,[†] Sami Jannin,*[,†] J. A. (Ton) Konter,[‡] Patrick Hautle,[‡] Ben van den Brandt,[‡] and Geoffrey Bodenhausen[†,§,‖,⊥]

[†]Institut des Sciences et Ingénierie Chimiques, Ecole Polytechnique Fédérale de Lausanne, EPFL, Batochime, 1015 Lausanne, Switzerland

[‡]Paul Scherrer Institute, CH-5232 Villigen, Switzerland

[§]Département de Chimie, Ecole Normale Supérieure, 24 Rue Lhomond, 75231, Paris Cedex 05, France

[‖]Université Pierre-et-Marie Curie, Paris, France

[⊥]CNRS, UMR 7203, Paris, France

**ABSTRACT:** Long-lived coherences (LLCs) in homonuclear pairs of chemically inequivalent spins can be excited and sustained during protracted radio frequency irradiation periods that alternate with brief windows for signal observation. Fourier transformation of the sustained induction decays recorded in a single scan yields NMR spectra with line-widths in the range $10 < \Delta\nu < 100$ mHz, even in moderately inhomogeneous magnetic fields. The resulting doublets, which are reminiscent of $J$-spectra, allow one to determine the sum of scalar and residual dipolar interactions in partly oriented media. The signal intensity can be boosted by several orders of magnitude by "dissolution" dynamic nuclear polarization (DNP).
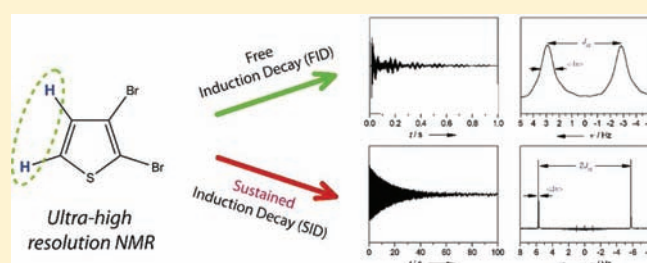
## INTRODUCTION

Most nuclear magnetic resonance (NMR) methods employ Fourier transformations of free induction decays (FIDs).[1] Although widely used, this approach suffers from homogeneous decay and imperfect homogeneity of the static magnetic field, so that it is challenging to achieve line-widths below 1 Hz.[2] Sophisticated NMR pulse sequences have been developed to achieve reasonable line-widths ($1 < \Delta\nu < 50$ Hz) in moderately inhomogeneous fields, exploiting cross relaxation effects,[3] observation in the earth's magnetic field,[4] or a spatial correlation between the static and radio frequency ($rf$) field profiles.[5] By combining refocusing and coherence transfer through couplings, one can obtain acceptable line-widths ($1 < \Delta\nu < 50$ Hz) even in very inhomogeneous fields ($\Delta\nu > 2$ kHz).[6] In systems with two scalar-coupled homonuclear spins $I = 1/2$ and $S = 1/2$, one can excite long-lived coherences (LLCs) that can have very long lifetimes $T_{LLC}$ and hence very narrow line-widths $\Delta\nu_{LLC} = 1/(\pi T_{LLC})$.[7−9] Their precession frequency is independent of offset (and hence of chemical shifts and inhomogeneous broadening) and is only determined by the sum of scalar and residual dipolar couplings ($T_{IS} = 2J_{IS} + D_{IS}$). So far, LLCs have only been observed indirectly in the manner of two-dimensional (2D) spectroscopy, either in combination with field cycling[7] or in high field.[8,9] This work describes a one-dimensional (1D) "on-the-fly" method where the $rf$ irradiation required to sustain the LLCs in high magnetic field is briefly interrupted at regular intervals, so that the LLCs can be temporarily observed as single-quantum coherences (SQCs). In contrast with conventional FIDs, the "sustained induction decays"

(SIDs) that are observed in this manner provide line-widths as narrow as $\Delta\nu_{LLC} = 14$ mHz even in poorly shimmed magnets ($\Delta\nu > 20$ Hz). This technique is fully compatible with signal enhancement by "dissolution" dynamic nuclear polarization (DNP).[10]

## PRINCIPLES

Long-lived coherences (LLCs) constitute a class of zero-quantum coherences that can be excited by extremely low frequency fields (ELFs) in a vanishing static field.[7] LLCs can also be excited in high fields by creating a state where the coherences $I_x$ and $-S_x$ have opposite phases, so that they can be locked by a continuous "sustaining" $rf$ field.[8,9] This $rf$ field in effect suppresses the chemical shifts, thus rendering the spins magnetically equivalent, so that their eigenstates can be classified according to "symmetrical" and "antisymmetrical" irreducible representations of the spin permutation group. LLCs span zero-quantum transitions between states of different symmetry. Their oscillatory decays can be subjected to a Fourier transformation, yielding doublets that are reminiscent of "$J$-spectroscopy".[11−13] The lifetimes $T_{LLC}$ of LLCs can be a factor $\kappa$ longer than the transverse relaxation times $T_2 = T_{SQC}$ of ordinary single-quantum coherences ($T_{LLC} = \kappa T_2$), so that the line-widths $\Delta\nu_{LLC} = 1/(\pi T_{LLC})$ can be narrower by a factor $\Delta\nu_{LLC}/\Delta\nu_{SQC} = 1/\kappa$. Depending on the role of extraneous relaxation mechanisms,[9] one can expect $\kappa \le 3$ in small molecules in the extreme
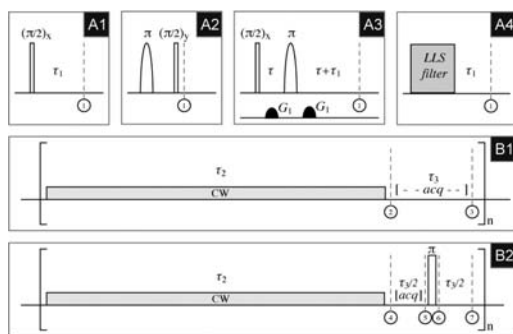
**Figure 1.** Pulse sequences for exciting and sustaining LLCs with "on the fly" observation of the magnetization in brief windows. One of the four preparation sequences A1–A4 allows one to create a density operator $\sigma = I_x - S_x$ (see text). Either of the two sequences B1 and B2 can be used to sustain the LLCs by CW irradiation and to acquire signals in the windows $\tau_3$ or $\tau_3/2$. The sustaining–acquisition blocks must be repeated $n$ times.

narrowing limit, and $\kappa \leq 9$ in the slow[14] motion limit typical of large molecules. In practice, we have observed $2.5 < \kappa < 4.3$ over a range of correlation times.[15]

The effects exploited in this work are closely related to those described by Hartmann and Hahn,[16] by Chingas et al.,[17] by Levitt,[18] and by Konrat et al.[19] In all cases (regardless of whether the transfer occurs via dipolar interactions in solids or via scalar couplings in liquids), there is an oscillatory to-and-fro motion between coherences associated with individual spins.

Generally speaking, LLCs should not be confused with long-lived states (LLSs), also known as singlet states (SS) if there are only two spins in the system. LLSs refer to populations of antisymmetric singlet states.[20–24] LLSs have lifetimes that can be much longer than LLCs ($T_{LLS} \gg T_{LLC}$), but do not have any oscillatory character and cannot give rise to $J$-spectra in the manner of LLCs. LLSs can be enhanced by "dissolution" DNP.[10,25]

If the oscillatory decays of LLCs are observed point-by-point in the manner of two-dimensional (2D) spectroscopy, they cannot be enhanced ("hyperpolarized") by "dissolution" DNP. Recently, several 2D experiments have been successfully converted into "ultrafast" versions that can be combined with "dissolution" DNP.[26,27] However, the continuous $rf$ field required to sustain LLCs is not compatible with current "ultrafast" schemes. In this work, we describe a novel one-dimensional (1D) method that is fully compatible with hyperpolarization techniques. In our experiment, the signals are observed during brief interruptions of the sustaining $rf$ field (scheme B1 in Figure 1). In the simplest version of the experiments, the windows are kept short, so that the evolution under chemical shifts, couplings, and transverse relaxation can be neglected (Figure 1, B1). In more sophisticated experiments, the sensitivity can be improved by making the windows somewhat longer, and by inserting $\pi$ refocusing pulses in these windows to refocus chemical shifts (scheme B2 in Figure 1).

The initial Boltzmann equilibrium populations, described by the density operator $\sigma = I_z + S_z$ (which may be enhanced by DNP), must be transformed into $\sigma = I_x - S_x$. Scheme A1 of Figure 1 starts with a nonselective $(\pi/2)_x$ pulse to excite the state $\sigma = -I_y - S_y$ followed by a delay $\tau_1 = 1/(2|\Delta\Omega_{IS}|)$, where $\Delta\Omega_{IS} = \Omega_I - \Omega_S$. Because the $rf$ carrier is positioned halfway between the two chemical shifts at $\omega_{rf} = (\Omega_I + \Omega_S)/2$, $\sigma = -I_y - S_y$ is transformed into $\sigma = I_x - S_x$ during the delay $\tau_1$. The precession under $J_{IS}$ in the interval $\tau_1$ can be neglected because $2\pi J_{IS} \ll \Delta\Omega_{IS}$. In scheme A2, a semiselective $\pi$ pulse applied to either $I$ or $S$ to invert the populations across either of

the two doublets is immediately followed by a nonselective $(\pi/2)_y$ pulse to excite $\sigma = I_x - S_x$.[8,9] In aqueous solutions, it may be necessary to suppress the intense HDO peak. Hence, scheme A3 uses an echo sequence $(\pi/2)_x - \tau - (\pi)_x^{(I,S)} - \tau$ with a band-selective refocusing pulse that acts on spins $I$ and $S$ but is too weak to refocus the solvent resonance. The two pulsed field gradients (PFGs) lead to dephasing of all magnetization components with offsets that lie outside the range of the band-selective refocusing pulse. Like in scheme A1, $\sigma = I_x - S_x$ is created after a delay $2\tau + \tau_1 = 2\tau + 1/(2|\Delta\Omega_{IS}|)$. Finally, scheme A4 uses a "long-lived state filter" as explained elsewhere.[15] The two latter schemes also have the advantage of avoiding possible radiation damping induced by large HDO signals, especially when enhanced by DNP.

Both schemes B1 and B2 in Figure 1 rely on a continuous-wave (CW) $rf$ field for "sustaining" or "locking" the LLC, to suppress the chemical shifts of spins $I$ and $S$, with a carrier $\omega_{rf} = (\Omega_I + \Omega_S)/2$ and an $rf$ amplitude that must be larger than the offsets $\omega_1 > |\Omega_I - \Omega_S|/2$. More sophisticated methods may also be used to sustain LLCs over greater bandwidths.[28] During $rf$ irradiation, the eigenstates are better described in the singlet–triplet base.[9] In this base, the density operator $\sigma = I_x - S_x$ can be written $\sigma = (|S_0\rangle\langle T_0| + |T_0\rangle\langle S_0|)$, that is, a zero-quantum coherence spanning the central triplet state $T_0 = N(|\alpha\beta\rangle + \langle\beta\alpha|)$ and the singlet state $S_0 = N(|\alpha\beta\rangle - \langle\beta\alpha|)$ where $N = 2^{-1/2}$. In the windows $\tau_3$ or $\tau_3/2$ where the $rf$ field is switched off, the density operator, described in the product base as single-quantum coherences $\sigma = I_x - S_x$, gives rise to signals that can be observed. In both schemes B1 and B2 in Figure 1, the LLCs are sustained during the intervals $\tau_2$, while the signals are detected in the windows $\tau_3$ or $\tau_3/2$. The sustain–observe cycles are repeated $n$ times, resulting in "sustained induction decays" (SIDs) with a total length $t^{max} = n\Delta t$ digitized at intervals $\Delta t = \tau_2 + \tau_3$ in schemes B1 or B2. The $\Delta t$ intervals are equivalent to the "dwell times" of ordinary free induction decays. The signals can be readily Fourier transformed, giving a frequency domain spectrum with a digital resolution that is determined by $1/t^{max}$ and a spectral width $1/\Delta t$ that should be larger than the total coupling $T = 2J + D$ if one wishes to avoid aliasing.

This type of "windowed acquisition" is reminiscent of solid-state NMR methods such as WAHUHA, MREV, and their numerous variants.[29,30] Recently, "windowed acquisition" has also been used for homonuclear dipolar decoupling with shaped rf pulses in the manner of DUMBO.[31] If the windows are too short, the signals can be perturbed by transient effects due to transmitter breakthrough, bearing in mind that the preamplifier must be protected during $rf$ irradiation, and that this protection must be removed in the windows. On the other hand, if the windows are too long, the single-quantum coherences $\sigma = I_x - S_x$ will decay through transverse $T_2$ relaxation, dephase in the inhomogeneous static field, and evolve under the chemical shifts and scalar couplings. With an analogue-to-digital converter (ADC) running at 500 kHz, we can acquire a sample point every 2 $\mu$s, and take averages over all points recorded in each interval $\tau_3$ of scheme B1 or in the first $\tau_3/2$ interval of scheme B2. Reducing the number of sampling points leads to a loss in signal-to-noise ratio. In practice, the dead time between the point where the CW $rf$ field is switched off, and where the signal can be observed is typically 3 $\mu$s, so that eight sampling points can be taken in each window if $\tau_3 = 20$ $\mu$s, or 498 points in each window if $\tau_3 = 1000$ $\mu$s. If the sustaining intervals in scheme B1 of Figure 1 are adjusted to keep a constant dwell time $\Delta t = \tau_2 + \tau_3 = 50$ ms so that a spectral width is $1/\Delta t = 20$ Hz or $\pm 10$ Hz, windows $\tau_3 = 20$ or 1000 $\mu$s lead to $rf$ duty cycles of 99.96% or 98%, respectively.
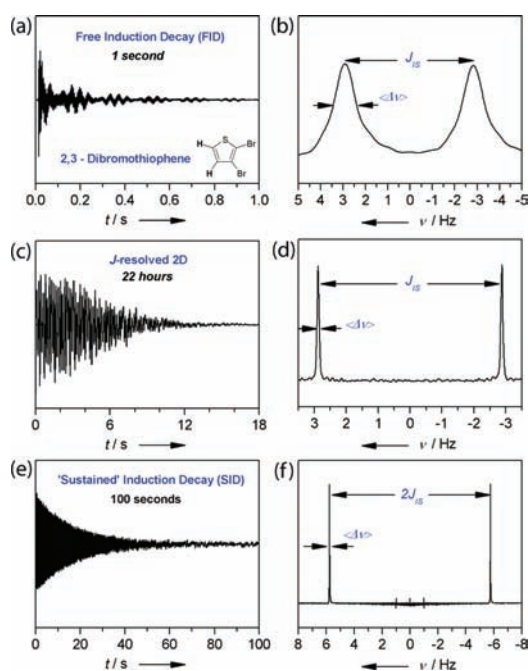
**Figure 2.** Examples of FIDs and SIDs recorded "on the fly" with their Fourier transforms. (a) Real part of a conventional "free induction decay" (FID) due to single-quantum coherences (SQCs) of the two protons of 2,3-dibromothiophene in a 20 mM isotropic solution in DMSO-$d_6$ with 30 mM ascorbic acid, measured at 11.7 T (500 MHz for protons) and 296 K. (b) Conventional Fourier transform of the FID in (a), showing a doublet with linewidths $\langle\Delta\nu\rangle \approx 1.5$ Hz and a splitting $J_{IS} \approx 5.8$ Hz. (c) Real part of the echo amplitude (note that the time scale was expanded by a factor 18 with respect to (a)) measured with conventional $J$-resolved $^1$H spectroscopy.[32] (d) Positive projection of the two-dimentional Fourier transform, showing a doublet with linewidths $\langle\Delta\nu\rangle \approx 70$ mHz and a splitting $J_{IS} \approx 5.77$ Hz. (e) Real part of the "sustained induction decay" (SID) acquired "on the fly" in a single scan (note that the time scale was expanded by a factor 100 with respect to (a)), arising from an LLC excited in the same sample with sequence A3 of Figure 1, sustained and observed with sequence B2. The parameters were $\tau_3/2 = 100$ $\mu$s, $\Delta t = \tau_2 + \tau_3 = 50$ ms, $rf$ amplitude of the CW sustaining field $\gamma B_1/(2\pi) = 4.5$ kHz, offsets $\Omega_I/(2\pi) = -\Omega_S/(2\pi) = 145$ Hz, the $rf$ carrier being set halfway between the two chemical shifts. (f) Spectrum obtained by a real Fourier transformation of the SID of (e), showing a doublet with linewidths $\langle\Delta\nu\rangle \approx 16.4$ mHz and a splitting $2J_{IS} \approx 11.5286$ Hz. If undesirable spin-locked $I_x + S_x$ terms had not been suppressed, they would give rise to peak at $\nu = 0$. The narrowest linewidths $\langle\Delta\nu\rangle = 14$ mHz (not shown) were observed with scheme B1, $\tau_3 = 30$ $\mu$s, and $\Delta t = \tau_2 + \tau_3 = 50$ ms.

During the irradiation intervals $\tau_2$, the coherence $Q_{LLC} = (|S_0\rangle\langle T_0| + |S_0\rangle\langle T_0|)$ evolves under the effect of the total coupling $T_{IS} = 2J_{IS} + D_{IS}$ and decays with the relaxation rate $R_{LLC} = 1/T_{LLC}$:

$$\frac{d}{dt} Q_{LLC} = -(R_{LLC} + i\pi T_{IS}) \cdot Q_{LLC} \tag{1}$$

In terms of the usual Cartesian product operators, this leads to:

$$\sigma_2 = [(I_x - S_x)\cos(\pi T_{IS}\tau_2) + (2I_yS_z - 2I_zS_y)\sin(\pi T_{IS}\tau_2)]\exp(-\tau_2 \cdot R_{LLC}) \tag{2}$$

This is consistent with our recent work,[9] but our initial paper[8] underestimated the effect of the couplings by a factor 2. During each window $\tau_3$ in the scheme B1 of Figure 1, the density



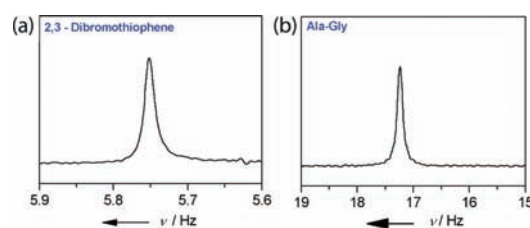**Figure 3.** (a) Zoom of Figure 2d, with $J_{IS}^{app} = 5764.3 \pm 0.2$ mHz and $\langle\Delta\nu\rangle = 16.4 \pm 0.1$ mHz. (b) Similar zoom of an "on the fly" LLC spectrum of the two diastereotopic protons of glycine in L-Ala-Gly, with $J_{IS}^{app} = 17\,236.5 \pm 0.2$ mHz and $\langle\Delta\nu\rangle = 115.0 \pm 0.7$ mHz.

operator evolves under the chemical shifts and again under the total coupling constant $T_{IS}$, albeit attenuated by a factor 2, and decays with the single-quantum relaxation rate $R_2 = 1/T_2$. The overall effect for each sustain-and-observe cycle $\Delta t = \tau_2 + \tau_3$ in scheme B1 can be written:

$$\sigma_3 = \cos(\Delta\Omega_{IS}/2 \cdot \tau_3)\exp(-\langle R\rangle\Delta t) \cdot [(I_x - S_x)\cos(\pi T_{IS}\Delta t')$$
$$+ (2I_yS_z - 2I_zS_y)\sin(\pi T_{IS}\Delta t')]$$
$$+ \sin(\Delta\Omega_{IS}/2 \cdot \tau_3)\exp(-\langle R\rangle\Delta t) \cdot [(I_y + S_y)\cos(\pi T_{IS}\Delta t')$$
$$- (2I_xS_z + 2I_zS_x)\sin(\pi T_{IS}\Delta t')] \tag{3}$$

where $\Delta t' = \tau_2 + \tau_3/2 = \Delta t - \tau_3/2$, reflecting the scaling of the total coupling constant when the $rf$ field is switched off. So we can define an apparent total coupling constant:

$$T_{IS}^{app} = T_{IS}\Delta t'/\Delta t \tag{4}$$

Using the notation $R_2 = R_{SQC} = \kappa R_{LLC}$ with $\kappa \leq 9$, the average decay rate $\langle R\rangle$ in eq 3 is

$$\langle R\rangle = \frac{1}{\Delta t}(\tau_2 R_{LLC} + \tau_3 R_2) = \frac{\tau_2 + \kappa\tau_3}{\tau_2 + \tau_3}R_{LLC} \tag{5}$$

For $\kappa = 3$, $\tau_2 = 49.98$ ms, and $\tau_3 = 20$ $\mu$s, this amounts to a mere 0.08% increase in the average relaxation rate and hence to a negligible contribution to the line-width. When the CW $rf$ field along the $x$-axis is switched on again, the differences $I_x - S_x$ and $2I_yS_z - 2I_zS_y$ resume their identity as LLCs, while the sum $I_y + S_y$ is spin-locked and decays with $R_{1\rho}$, and the sum $2I_xS_z + 2I_zS_x$ is dephased under the effect of the $rf$ field inhomogeneity. With a chemical shift difference $\Delta\Omega_{IS}/(2\pi) = 300$ Hz, we have $\cos(\Delta\Omega_{IS}\tau_3) = 0.9993 \sim 1$. This infinitesimal "leakage" of the LLC seems negligible, but it is amplified as the sustain−observe sequence is repeated $n$ times with $\cos(\Delta\Omega_{IS}\tau_3)^n$ so that $\cos(\Delta\Omega_{IS}\tau_3)^{100} = 0.936$, thus affecting the decay of the LLC. The resulting time domain signals sampled at intervals $\Delta t$ are

$$I(n\Delta t) = I_0 \cos(\pi T_{IS}n\Delta t')$$
$$\times \exp\left[-n\Delta t \cdot \left(\frac{\tau_2}{\tau_2 + \tau_3} \cdot R_{LLC} + \frac{\tau_3}{\tau_2 + \tau_3} \cdot R_2\right)\right]\cos(\Delta\Omega_{IS}\tau_3)^n$$
$$= I_0 \cos(\pi T_{IS}^{app}n\Delta t)\exp(-n\Delta t \cdot \langle R\rangle)\cos(\Delta\Omega_{IS}\tau_3)^n \tag{6}$$

However, when $\tau_3$ is long, the "leakage" can become significant: for $\tau_3 = 1$ ms, $\cos(\Delta\Omega_{IS}\tau_3) = 0.9553$, and hence $\cos(\Delta\Omega_{IS}\tau_3)^{100} = 0.01$, so that the scheme described below is to be preferred.

To suppress contributions from $I_y + S_y$ and $2I_xS_z + 2I_zS_x$, scheme B2 uses a $\pi$ pulse in the middle of each window to refocus the chemical shifts. As a result, the density operator at the end of
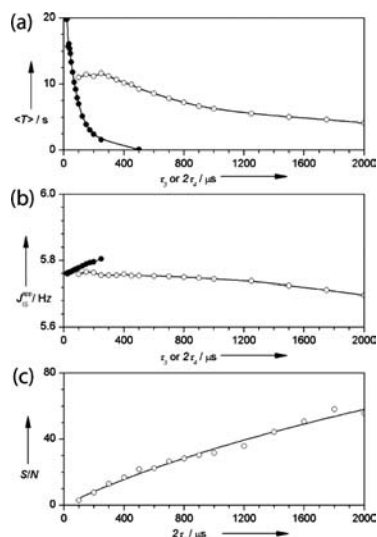
**Figure 5.** "On the fly" LLCs in an inhomogeneous magnetic field. (a) Conventional (single-quantum) NMR spectra of the same sample of 2,3-dibromothiophene as in Figure 2, obtained by Fourier transformation of an FID measured at 11.7 T (500 MHz for protons), with the magnet shimmed to yield a line-width $\Delta\nu \approx 1.2$ Hz (black line) and deliberately deshimmed to yield a line-width $\Delta\nu \approx 20$ Hz (blue line). (b) LLC spectra observed "on the fly" of the same sample in the same homogeneous ($\langle\Delta\nu_{LLC}\rangle = 17.5 \pm 0.2$ mHz and $J_{IS}^{app} = 5.741$ Hz $\pm$ 0.1 mHz) and inhomogeneous fields ($<\Delta\nu_{LLC}> = 22.8 \pm 0.4$ mHz and $J_{IS}^{app} = 5.744$ Hz $\pm$ 0.2 mHz). In a poorly shimmed magnetic field, some broadening (+5.3 mHz) and a slight error in $J_{IS}^{app}$ (+3 mHz) are thus observed. The areas of the peaks are identical. The LLCs were excited with sequence A3 and sustained and observed with sequence B2 of Figure 1 with the following parameters: $\tau_4 = 500\,\mu s$, $\Delta t = \tau_2 + \tau_3 = 50$ ms, rf amplitude of CW sustaining field $\gamma B_1/(2\pi) = 4.5$ kHz.



**Figure 4.** Average lifetimes, apparent scalar couplings, and signal-to-noise ratios. (a) Average lifetimes $\langle T\rangle = 1/\langle R\rangle$ (see eq 5) in the same sample of 2,3-dibromothiophene as in Figure 2, measured as a function of the duration of the windows $\tau_3$ in scheme B1 without refocusing pulses ($\bullet$) and in scheme B2 using $\pi$ refocusing pulses ($\circ$), averaging signals sampled at a rate of 500 kHz in each interval, and adapting $\tau_2$ to keep a constant dwell time $\Delta t = 50$ ms. The lines are drawn to guide the eye. (b) Apparent scalar coupling constant $J_{IS}^{app}$ in 2,3-dibromothiophene observed as a function of the duration of $\tau_3$ in method B1 ($\bullet$) or in scheme B2 ($\circ$) with a constant dwell time $\Delta t = 50$ ms. (c) Signal-to-noise ratio (S/N) for the same sample of 2,3-dibromothiophene determined with scheme B2 with $100\,\mu s < \tau_3 < 2$ ms. The black line shows a fit to the function $S/N \approx \tau_3^{1/2}$.

each window $\tau_3$ in scheme B2 is:

$$\sigma_7 = [(I_x - S_x)\cos(\pi T_{IS}\Delta t') \\ + (2I_yS_z - 2I_zS_y)\sin(\pi T_{IS}\Delta t')]\exp(-\langle R\rangle\Delta t) \quad (7)$$

The resulting time domain signals sampled at intervals $\Delta t$ are:

$$I(n\Delta t) = I_0 \cos(\pi T_{IS}n\Delta t') \\ \times \exp\left[-n\Delta t\cdot\left(\frac{\tau_2}{\tau_2+\tau_3}\cdot R_{LLC} + \frac{\tau_3}{\tau_2+\tau_3}\cdot R_2\right)\right] \\ = I_0 \cos(\pi T_{IS}^{app}n\Delta t)\exp(-n\Delta t\cdot\langle R\rangle) \quad (8)$$

## ■ EXPERIMENTAL EVIDENCE

Figure 2e shows an SID that can be compared to the FID presented in Figure 2a and to the modulated echo decay of Figure 2c. The three signals stem from the two protons in an isotropic solution of 2,3-dibromothiophene (20 mM in DMSO-$d_6$ with 30 mM ascorbic acid[33] to scavenge paramagnetic oxygen), recorded with a simple $\pi/2$ pulse (Figure 2a), in a J-resolved 2D manner[32] (Figure 2c), and with "on the fly" LLCs in windows $\tau_3/2 = 100\,\mu s$ with scheme B2 (Figure 2e). Their Fourier transforms are presented in Figure 2b, d, and f, respectively. The LLCs "SID" signal is described by eq 8 and slowly decays with a time-constant $\langle T\rangle = 1/\langle R\rangle = 19.9$ s. Its Fourier transforms (Figures 2f and 3a) show two lines at $\nu = \pm J_{IS}$
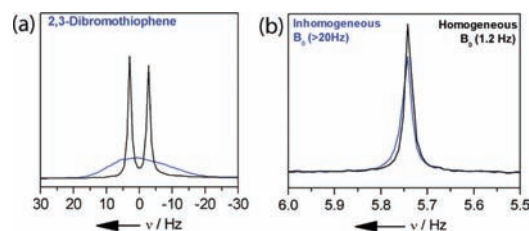
separated by $2J_{IS}$ with line-widths $\langle\Delta\nu\rangle = 1/(\pi\langle T\rangle) = 16.4$ mHz (resolution enhanced by a factor $\varepsilon_\Delta = \nu/\langle\Delta\nu\rangle \approx 180$ and 8.5 with respect to conventional FID and echo modulation, respectively). The fact that the couplings are twice as effective in the rotating frame than in the laboratory frame is reminiscent of total correlation spectroscopy ("TOCSY").[34] Note that the antiphase terms $2I_yS_z - 2I_zS_y$ cannot induce any signals in the orthogonal channel, so that we have a case of pure amplitude (rather than phase) modulation. The "on the fly" LLC spectrum of the two diastereotopic protons of glycine in L-Ala-Gly is shown in Figure 3b.

Figure 4a shows how the insertion of refocusing pulses in the windows allows one to eliminate the effects of chemical shifts. For longer windows $100\,\mu s < \tau_3 < 2$ ms, scheme B2 provides longer decays and hence narrower line-widths. Note that the narrowest lines are obtained, albeit at the expense of sensitivity, with scheme B1 with very short windows (typically $\tau_3 = 20\,\mu s$). Figure 4b shows how refocusing allows one to obtain an accurate measurement of scalar couplings $J_{IS}$ (or total couplings $T_{IS}$ in anisotropic media) even for long windows $\tau_3$. (The slight decrease in $J_{IS}^{app}$ for long $\tau_3$ is described by eq 4). Finally, Figure 4c shows how longer windows $\tau_3$, which allow one to average over a larger number of data points in each window, result in improved signal-to-noise ratios, which are proportional to $\tau_3^{1/2}$ as expected.

**"On the Fly" LLCs in Inhomogeneous $B_0$.** In principle, the evolution of LLCs is immune to the inhomogeneity of the magnetic field if one uses scheme B2 of Figure 1. We should remember however that all excitation schemes A1–A4 of Figure 1 require one to distinguish the chemical shifts of the two spins I and S, but not their mutual coupling constant. The methods can thus tolerate a moderate inhomogeneity of the static field, as long as the line-widths fulfill the condition $\Delta\nu^* = 1/(\pi T_2^*) < \Delta\Omega_I$. Figure 5 shows how a deliberate missetting of the shim currents ($z_1$, $z_2$, $z_3$, $x$, $y$, $z_0x$, and $z_0y$) to broaden the line-widths to about $\Delta\nu^* = 20$ Hz has little effect on the line-widths $\langle\Delta\nu\rangle$ of the LLCs and the apparent scalar couplings $J_{IS}^{app}$ (+5.3 and +3 mHz, respectively). Ex-situ NMR[4,5] and MRI in moderately inhomogeneous fields (e.g., in the vicinity of
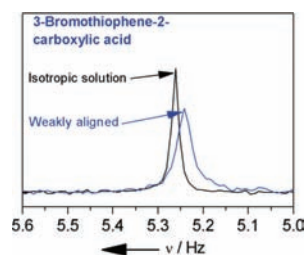
**Figure 6.** "On the fly" LLCs in a weakly oriented media. LLC spectra observed "on the fly" of 3-bromothiophene-2-carboxylic acid in a (1:1) $D_2O$/DMSO-$d_6$ with and without addition of a very small amount (0.25%) of $C_5E_{12}$ (blue and black lines, respectively) measured at $B_0 =$ 11.7 T (500 MHz for protons) and $T$ = 300 K. The isotropic solution shows $J_{IS}^{app}$ = 5252.0 ± 0.2 mHz and $\langle \Delta \nu \rangle \approx$ 18.5 mHz, whereas the weakly aligned medium gives $T_{IS}^{app} = 2J_{IS}^{app} + D_{IS}^{app}$ = 10482.6 ± 0.4 mHz and $\langle \Delta \nu \rangle \approx$ 40.0 mHz, hence $D_{IS}^{app}$ = 21.4 ± 0.8 mHz. The LLCs were excited with sequence A3 and sustained and observed with sequence B2 of Figure 1 with the following parameters: $\tau_3/2$ = 500 $\mu$s, $\Delta t$ = $\tau_2 + \tau_3$ = 50 ms, rf amplitude of CW sustaining field $\gamma B_1/(2\pi)$ = 4.5 kHz.
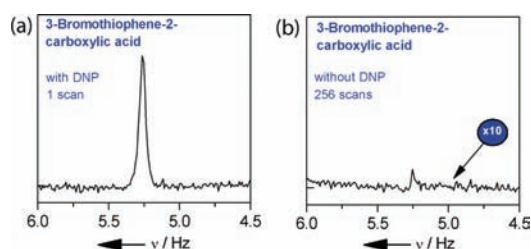


**Figure 7.** Hyperpolarized "on the fly" LLC spectrum of 3-bromothio-phene-2-carboxylic acid, showing a 300-fold enhancement of the signal intensity. (a) The sample consisted of 20 $\mu$L of a 50 mM solution of 3-bromothiophene-2-carboxylic acid in a 3:2 DMSO-$d_6$/$D_2O$ (v/v) mixture, doped with 30 mM TEMPO, rapidly frozen, immersed in a field of 3.35 T, hyperpolarized by 30 mW microwave irradiation at 93.89 GHz at 1.2 K during 300 s, and dissolved with 3 mL of preheated $D_2O$ to a final concentration of 250 $\mu$M 3-bromothiophene-2-carboxylic acid. The hyperpolarized sample was rapidly transferred to $B_0$ = 11.7 T (500 MHz for protons) at $T$ = 296 K, and the LLC was then excited with sequence A3, sustained, and observed with sequence B2 of Figure 1 with the following parameters: $\tau_3/2$ = 100 $\mu$s, $\Delta t$ = $\tau_2 + \tau_3$ = 50 ms, rf amplitude of CW sustaining field $\gamma B_1/(2\pi)$ = 4.5 kHz, offsets $\Omega_I/(2\pi) = -\Omega_S/(2\pi)$ = 103 Hz, the rf carrier being set halfway between the two chemical shifts. (b) Thermal equilibrium signal (i.e., without DNP) of the same sample measured with the same parameters, but with 256 scans and multiplied by a factor 10.

discontinuities of the magnetic susceptibility) may benefit from this property.

**"On the Fly" LLCs To Measure Very Weak Alignments.** Very weak molecular alignments, yielding minute residual dipolar couplings (RDC's) in the millihertz range, can be readily resolved with our method. Figure 6 shows the "on the fly" LLC spectra of two solutions of 3-bromothiophene-2-carboxylic acid in (1:1) $D_2O$/DMSO-$d_6$, with and without addition of a 0.25% pen-taethylene glycol monododecyl ether ($C_{12}E_5$). The very weak alignment of the solute gives rise to a net RDC with $D_{IS}^{app}$ = −21.4 ± 0.8 mHz. The order parameter of the $r_{HH}$ vector can be estimated to be $S \leq (1.01 \pm 0.04) \; 10^{-5}$ (assuming $r_{HH}$ = 2.662 Å like in thiophene,[35] with the average H−H vector oriented along $B_0$, i.e., $\theta$ = 0). This is the first time residual dipolar couplings are considered in LLC experiments, in addition to scalar couplings. In

high field, the corresponding Hamiltonians have the same form. Further work is in progress to determine the effects of RDCs on the homogeneous and inhomogeneous linewidths of LLCs.

**Hyperpolarized LLCs.** Because LLC spectra can be recorded in a single scan, they can be boosted by "dissolution" DNP. Spectra of a 20 $\mu$L solution of 50 mM 2,3-dibromothiophene dissolved in a 3:2 DMSO-$d_6$/$D_2O$ (v/v) mixture doped with 30 mM TEMPOL are compared in Figure 7 with and without hyperpolarization by "dissolution" DNP (see Methods). The dissolution, transfer, and injection required 3.2 s. After an additional 3 s of settling time in the NMR tube, some bubbles and convection cannot be ruled out. These tend to broaden ordinary (single-quantum) line-widths, but have little effect on LLC spectra. The LLCs were excited, sustained, and observed with sequences A3 and B2 of Figure 1. The enhancement was $\varepsilon_{DNP} \approx$ 300. It may be possible to improve this performance by preventing losses of the proton polarization due to relaxation in low fields during the voyage.[36]

## ■ CONCLUSION

Ultra high-resolution spectra of long-lived coherences (LLCs) can be obtained "on the fly" in one-dimensional fashion by time-shared "windowed acquisition". This allows one to determine very accurate total couplings $T = 2J + D$. The method can be applied to either isotropic or anisotropic phases, providing ultra high resolution even in moderately inhomogeneous magnetic fields, and the signals can be enhanced by "dissolution" DNP. The technique has been applied to pairs of spins in this study, but we intend to extend the scope of application of "on the fly" LLCs in the near future to multiple spin systems ($N > 2$) with broad-band excitation and detection (replacing CW by composite pulses) of several LLCs in the same molecule or in mixtures. Because inhomogeneous fields are not detrimental to LLCs, ex situ or in-cell studies should be readily feasible with unprece-dented line-widths, and because the long lifetimes of LLCs are exquisitely sensitive to the presence of paramagnetic species,[33] we believe they should be a sensitive probe for the detection paramagnetic oxygen.

## ■ METHODS

**Sample Preparation.** DNP sample: A 20 $\mu$L solution of 50 mM 3-bromothiophene-2-carboxylic acid (97%, Aldrich) was dissolved in a 3:2 mixture of DMSO-$d_6$/$D_2O$ (v/v) (99.98%, Aldrich) doped with 30 mM 4-hydroxy-2,2,6,6-tetramethylpiperidine 1-oxyl (TEMPOL) (purum, ≥97.0%, Fluka). The freshly prepared mixture was rapidly frozen in liquid nitrogen to form 10 $\mu$L beads. Ascorbate scavenger: A 3 M $D_2O$ solution of sodium L-ascorbate (≥99%, Aldrich) was prepared and rapidly frozen in liquid nitrogen (10 $\mu$L beads). Dibromothiophene sample: A 20 mM isotropic solution of 2,3-dibromothiophene (98% Aldrich) in DMSO-$d_6$ with addition of 30 mM L-ascorbic acid (BioXtra, ≥99.0%, Sigma) for scavenging paramagnetic oxygen was prepared and sealed in a 5 mm NMR tube. Aligned media: Two 50 mM solutions of 3-bromothiophene-2-carboxylic acid in a (1:1) $D_2O$/DMSO-$d_6$ mixture with addition of 30 mM L-ascorbic acid for scavenging paramagnetic oxygen were prepared, one with and the other without addition of 0.25% of pentaethylene glycol monododecyl ether ($C_{12}E_5$, Sigma ≥98%) for partial alignment, and sealed in 5 mm NMR tubes. Peptide sample: A 0.5 M solution of L-ala-gly (Sigma) in $D_2O$ with addition of 30 mM sodium L-ascorbate (≥99%, Aldrich) was prepared and sealed in a 5 mm NMR tube. All chemicals were used without further purification.

**Hyperpolarization.** DNP was performed by thermal mixing at 1.2 K and 3.35 T in a home-built "dissolution" DNP polarizer[37−39] by applying a CW microwave irradiation at $f_{\mu w}$ = 93.89 GHz and $P_{\mu w}$ = 30 mW for 5 min. The DNP buildup of $^1$H magnetization is fast ($\tau_{DNP} \approx$ 120 s) and yields high proton spin polarization P($^1$H) ≈ 20−40% depending on sample composition.[40] The 20 μL of frozen beads of the polarized sample, together with 90 μL of frozen beads of a 3 M $D_2O$ solution of sodium ascorbate, were rapidly dissolved with 3 mL of preheated $D_2O$ (T = 440 K and P = 1.2 MPa) and intimately mixed within 700 ms, transferred in 1.5 s to a 11.7 T Bruker magnet through a 1.5 mm inner diameter PTFE tube pressurized with helium gas at 0.6 MPa, and allowed to settle for 0.5 s, prior to injection into a prelocked NMR tube, which required another 0.5 s. After a further 3 s settling time in the NMR tube to allow turbulences to slow, the LLC was excited, sustained, and observed with the sequences A3 and B2 of Figure 1.

**NMR Measurements.** NMR measurements were performed on an UltraShield 500 MHz Avance Bruker spectrometer equipped with an Inverse 5 mm CryoProbe. The "on the fly" LLC pulse program and excitation/acquisition sequences were designed and performed with TopSpin 2.1. The Bruker pulse program is available on request.

## ■ AUTHOR INFORMATION

**Corresponding Author**
sami.jannin@epfl.ch

## ■ ACKNOWLEDGMENT

## ■ REFERENCES

(1) Ernst, R. R.; Anderson, W. A. *Rev. Sci. Instrum.* **1966**, *37*, 93.

(2) Allerhand, A.; Addleman, R. E.; Osman, D. *J. Am. Chem. Soc.* **1985**, *107*, 5809−5810.

(3) Balbach, J. J.; Conradi, M. S.; Cistola, D. P.; Tang, C. G.; Garbow, J. R.; Hutton, W. C. *Chem. Phys. Lett.* **1997**, *277*, 367−374.

(4) Appelt, S.; Kuhn, H.; Hasing, F. W.; Blumich, B. *Nat. Phys.* **2006**, *2*, 105−109.

(5) Meriles, C. A.; Sakellariou, D.; Heise, H.; Moule, A. J.; Pines, A. *Science* **2001**, *293*, 82−85.

(6) Pelupessy, P.; Rennella, E.; Bodenhausen, G. *Science* **2009**, *324*, 1693−1697.

(7) Pileio, G.; Carravetta, M.; Levitt, M. H. *Phys. Rev. Lett.* **2009**, *103*, 083002.

(8) Sarkar, R.; Ahuja, P.; Vasos, P. R.; Bodenhausen, G. *Phys. Rev. Lett.* **2010**, *104*, 053001.

(9) Sarkar, R.; Ahujab, P.; Vasos, P. R.; Bornet, A.; Wagnières, O.; Bodenhausen, G. *Prog. Nucl. Magn. Reson. Spectrosc.* **2011**, *59*, 83−90.

(10) Ardenkjaer-Larsen, J. H.; Fridlund, B.; Gram, A.; Hansson, G.; Hansson, L.; Lerche, M. H.; Servin, R.; Thaning, M.; Golman, K. *Proc. Natl. Acad. Sci. U.S.A.* **2003**, *100*, 10158−10163.

(11) Freeman, R.; Hill, H. D. W. *Dynamic Nuclear Magnetic Resonance Spectroscopy*; Academic Press: New York, 1975; Vol. 36.

(12) Bodenhausen, G.; Freeman, R.; Turner, D. L. *J. Chem. Phys.* **1976**, *65*, 839−840.

(13) Bodenhausen, G.; Freeman, R.; Morris, G. A.; Turner, D. L. *J. Magn. Reson.* **1977**, *28*, 17−28.

(14) Pelupessy, P.; Duma, L.; Bodenhausen, G. *J. Magn. Reson.* **2008**, *194*, 169−174.

(15) Bornet, A.; Sarkar, R.; Bodenhausen, G. *J. Magn. Reson.* **2010**, *206*, 154−156.

(16) Hartmann, S. R.; Hahn, E. L. *Phys. Rev.* **1962**, *128*, 2042.

(17) Bertrand, R. D.; Moniz, W. B.; Garroway, A. N.; Chingas, G. *J. Am. Chem. Soc.* **1978**, *100*, 5227−5229.

(18) Levitt, M. H. *J. Chem. Phys.* **1991**, *94*, 30−38.

(19) Konrat, R.; Burghardt, I.; Bodenhausen, G. *J. Am. Chem. Soc.* **1991**, *113*, 9135−9140.

(20) Carravetta, M.; Johannessen, O. G.; Levitt, M. H. *Phys. Rev. Lett.* **2004**, *92*, 153003−153007.

(21) Carravetta, M.; Levitt, M. H. *J. Chem. Phys.* **2005**, *122*, 214505.

(22) Sarkar, R.; Vasos, P. R.; Bodenhausen, G. *J. Am. Chem. Soc.* **2007**, *129*, 328−334.

(23) Pileio, G.; Levitt, M. H. *J. Chem. Phys.* **2009**, *130*, 214501.

(24) Ahuja, P.; Sarkar, R.; Vasos, P. R.; Bodenhausen, G. *ChemPhysChem* **2009**, *10*, 2217−2220.

(25) Vasos, P. R.; Comment, A.; Sarkar, R.; Ahuja, P.; Jannin, S.; Ansermet, J. P.; Konter, J. A.; Hautle, P.; van den Brandt, B.; Bodenhausen, G. *Proc. Natl. Acad. Sci. U.S.A.* **2009**, *106*, 18475−18479.

(26) Frydman, L.; Blazina, D. *Nat. Phys.* **2007**, *3*, 415−419.

(27) Pelupessy, P. *J. Am. Chem. Soc.* **2003**, *125*, 12345−12350.

(28) Sarkar, R.; Ahuia, P.; Moskau, D.; Vasos, P. R.; Bodenhausen, G. *ChemPhysChem* **2007**, *8*, 2652−2656.

(29) Waugh, J. S.; Huber, L. M.; Haeberlen, U. *Phys. Rev. Lett.* **1968**, *20*, 180.

(30) Rhim, W. K.; Elleman, D. D.; Vaughan, R. W. *J. Chem. Phys.* **1973**, *58*, 1772−1773.

(31) Lesage, A.; Sakellariou, D.; Hediger, S.; Elena, B.; Charmont, P.; Steuernagel, S.; Emsley, L. *J. Magn. Reson.* **2003**, *163*, 105−113.

(32) Aue, W. P.; Karhan, J.; Ernst, R. R. *J. Chem. Phys.* **1976**, *64*, 4226−4227.

(33) Miéville, P.; Ahuja, P.; Sarkar, R.; Jannin, S.; Vasos, P. R.; Gerber-Lemaire, S.; Mishkovsky, M.; Comment, A.; Gruetter, R.; Ouari, O.; Tordo, P.; Bodenhausen, G. *Angew. Chem., Int. Ed.* **2010**, *49*, 6182−6185.

(34) Braunschweiler, L.; Ernst, R. R. *J. Magn. Reson.* **1983**, *53*, 521−528.

(35) Bak, B.; Christensen, D.; Hansen-Nygaard, L.; Rastrup-Andersen, J. *J. Mol. Spectrosc.* **1961**, *7*, 58−63.

(36) Miéville, P.; Jannin, S.; Bodenhausen, G. *J. Magn. Reson.* **2011**, *210*, 137−140.

(37) Comment, A.; van den Brandt, B.; Uffmann, K.; Kurdzesau, F.; Jannin, S.; Konter, J. A.; Hautle, P.; Wenckebach, W. T. H.; Gruetter, R.; van der Klink, J. J. *Concepts Magn. Reson., Part B* **2007**, *31B*, 255−269.

(38) Comment, A.; van den Brandt, B.; Uffmann, K.; Kurdzesau, F.; Jannin, S.; Konter, J. A.; Hautle, P.; Wenckebach, W. T.; Gruetter, R.; van der Klink, J. J. *Appl. Magn. Reson.* **2008**, *34*, 313−319.

(39) Jannin, S.; Comment, A.; Kurdzesau, F.; Konter, J. A.; Hautle, P.; van den Brandt, B.; van der Klink, J. J. *J. Chem. Phys.* **2008**, *128*, 241102.

(40) Kurdzesau, F.; van den Brandt, B.; Comment, A.; Hautle, P.; Jannin, S.; van der Klink, J. J.; Konter, J. A. *J. Phys. D: Appl. Phys.* **2008**, *41*, 155506.

## ■ NOTE ADDED AFTER ASAP PUBLICATION

Corrections were made to equation 1 and the text following equations 5 and 6. This reposted ASAP September 12, 2011.

15649

dx.doi.org/10.1021/ja2052792 |*J. Am. Chem. Soc.* 2011, 133, 15644−15649